

Chapter 1

Solar Energetic Particles and Space Weather: Science and Applications

Olga E. Malandraki and Norma B. Crosby

Abstract This chapter provides an overview on solar energetic particles (SEPs) and their association to space weather, both from the scientific as well as from the applications perspective. A historical overview is presented on how SEPs were discovered in the 1940s and how our understanding has increased and evolved since then. Current state-of-the-art based on unique measurements obtained in the 3-dimensional heliosphere (e.g. by the Ulysses, ACE, STEREO spacecraft) and their analysis is also presented. Key open questions on SEP research expected to be answered in view of future missions that will explore the solar corona and inner heliosphere are highlighted. This is followed by an introduction to why SEPs are studied, describing the risks that SEP events pose on technology and human health. Mitigation strategies for solar radiation storms as well as examples of current SEP forecasting systems are reviewed, in context of the two novel real-time SEP forecasting tools developed within the EU H2020 HESPERIA project.

1.1 Science

1.1.1 *Historical Perspective of Solar Energetic Particle (SEP) Events*

It is widely accepted that protons, electrons, and heavier nuclei such as He-Fe are accelerated from a few keV up to GeV energies in at least two distinct locations, namely the solar flare and the coronal mass ejection (CME)-driven interplanetary (IP) shock. The particles observed in IP space and near Earth are commonly referred to as solar energetic particles (SEPs). Those accelerated at flares are known as

O.E. Malandraki (✉)
National Observatory of Athens, IAASARS, Athens, Greece
e-mail: omaland@noa.gr

N.B. Crosby
Royal Belgian Institute for Space Aeronomy, Brussels, Belgium
e-mail: Norma.Crosby@aeronomie.be

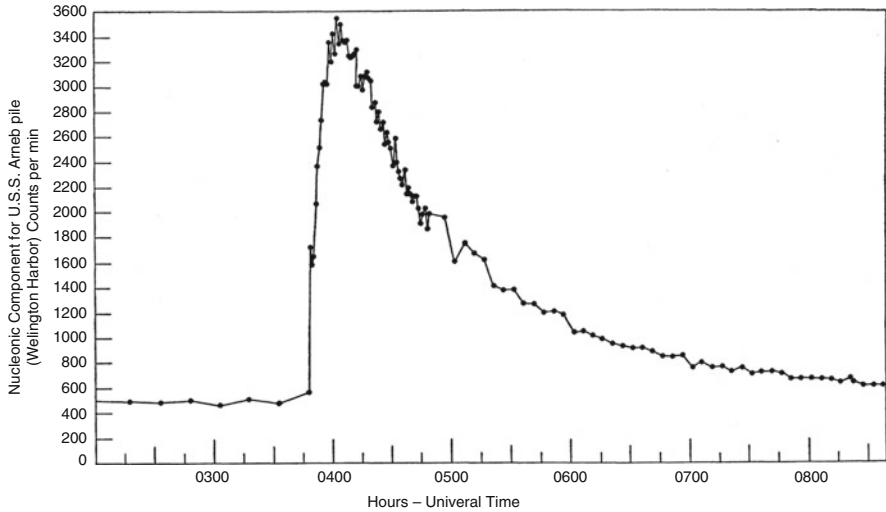


Fig. 1.1 Early observation of a solar energetic particle event (Reproduced from Meyer et al. 1956, permission for reuse from publisher American Physical Society for both print and electronic publication)

impulsive SEP events, particle populations accelerated by near-Sun CME-shocks are termed as gradual SEP events, and those associated with CME shocks observed near Earth are known as energetic storm particle (ESP) events (Desai and Giacalone 2016).

The first SEP event observations extending up to GeV energies were made with ground-based ionization chambers and neutron monitors in the mid 1940s (Forbush 1946). One early event is shown in Fig. 1.1. Until the mid-1990s the so-called ‘solar flare myth’ scenario was prevalent, in which large solar flares were considered to be the primary cause of major energetic particle events observed at 1 AU (Gosling 1993). However, Wild et al. (1963) had reviewed radio observations and on the basis of the slow-drifting type II bursts observed in close association with the SEP events, proposed an alternative view for the particle acceleration at magnetohydrodynamic shock waves, typically accompanying the flares.

By the end of the 1990s a two-class paradigm of SEP events (see Fig. 1.2) had been generally accepted (e.g. Reames 1999). The flare-related impulsive events lasted a few hours and were typically observed when the observer was magnetically connected to the flare site, were electron-rich and associated with type III radio bursts. These events also had ${}^3\text{He}/{}^4\text{He}$ ratios enhanced by factors 10^3 – 10^4 , enhanced Fe/O ratios by a factor of 10 over the nominal coronal values, and Fe ionization states of up to ~ 2 . On the other hand, the gradual events lasted several days, had larger fluences, and were attributed to be a result of diffusive acceleration at CME-driven coronal and IP shocks. They were proton-rich, had average Fe/O ratios of 0.1 and Fe ionization states of 14 and were associated with type II radio bursts (e.g. Cliver 2000; Reames 2013).

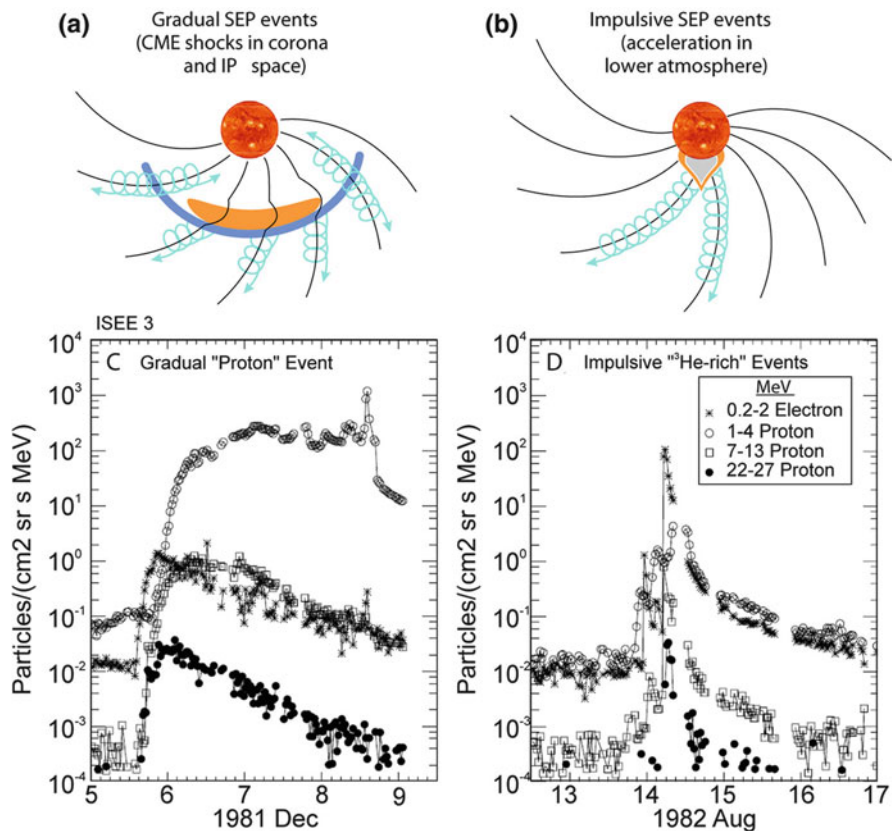


Fig. 1.2 The two-class paradigm of SEP events is presented (a) the gradual SEP events occur as a result of diffusive acceleration at CME-driven coronal and IP shocks and populate interplanetary magnetic field (IMF) lines over a large longitudinal extent (b) the impulsive SEP events which are produced by solar flares and which populate only those IMF lines well-connected to the flare site. Comparison of intensity-time profiles of electrons and protons in ‘pure’, (c) gradual and (d) impulsive SEP events. The gradual event is a disappearing—filament event with a CME but no impulsive flare. The impulsive events come from a series of flares with no CMEs (Reproduced from Desai and Giacalone 2016, permission for reuse from publisher Springer for both print and electronic publication)

Since then, observations have indicated that there are ‘hybrid’ or mixed event cases, where both mechanisms appear to contribute, with one accelerating mechanism operating in the flare while the other operates at the CME-driven shock (Kallenrode 2003). Such hybrid events may result from the re-acceleration of remnant flare suprathermals by shock waves (Mason et al. 1999; Desai et al. 2006) or from the interaction of CMEs (Gopalswamy et al. 2002). It is noteworthy however, that based on large enhancements in the Fe/O during the initial phases of two large SEP events observed by Wind and Ulysses when the two spacecraft (s/c) were separated by 60° in longitude (Tylka et al. 2013) argued that the initial Fe/O enhancements cannot be cited as evidence for a direct flare component, but instead

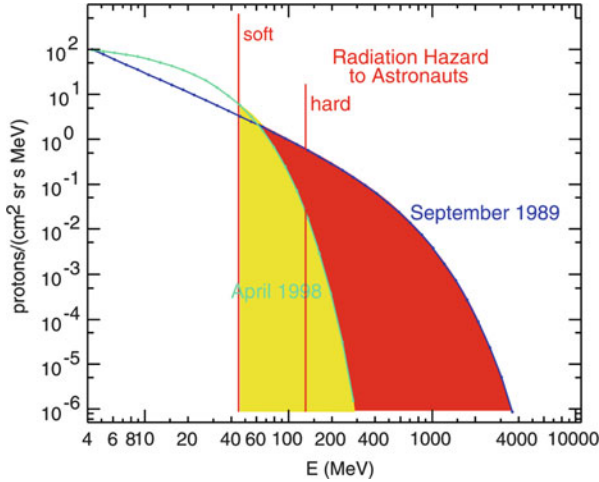


Fig. 1.3 Proton spectra of the SEP events of April 1998 (*green*, Tylka et al. 2000) and September 1989 (*blue*, Lovell et al. 1998) are compared. In *yellow* the hazardous portion of the spectrum during the April 1998 event is highlighted. The region of additional hazardous radiation from the September 1989 event is shaded *red* (Reproduced from Reames 2013, permission for reuse from publisher Springer for both print and electronic publication)

they are better understood as a transport effect, driven by the different mass-to-charge ratios of Fe and O.

High-energy protons in the largest SEP events can pose significant radiation hazards for astronauts and technological systems in space, particularly beyond the Earth's protective magnetic field (National Research Council (NCR) 2008; Cucinotta et al. 2010; Xapsos et al. 2012) (see Sect. 1.2 for more details).

Protons of ~ 150 MeV are considered as 'hard' radiation since they are very difficult to shield against. Essentially most of the radiation risk of humans in space from SEPs is due to proton intense fluxes of above ~ 50 MeV, i.e. 'soft' radiation, the energy at which protons begin to penetrate spacesuits and s/c housing. Figure 1.3 compares the proton energy spectra for two large SEP events, presenting typical knee energies of soft and hard radiation SEP events. The most important factor in the radiation dose and depth of penetration of the ions is the location of the energy spectral knee. In yellow in Fig. 1.3, the hazardous part of the spectrum for the April 1998 event is shown, whereas the red shaded area denotes the region of the additional hazardous radiation from the September 1989 event. In the April 1998 event the spectrum rolls over much more steeply at high energies, whereas in the September 1989 event the spectral knee occurred between ~ 200 and 300 MeV. Events with higher roll-over energies have significantly higher proton intensities above ~ 100 MeV and can constitute a severe radiation hazard to astronauts (Reames 2013). In fact during the September 1989 event, even an astronaut behind 10 g cm^{-2} of material would receive a dose of ~ 40 mSv. The annual dose limit for a radiation worker in the United States is 20 mSv (Zeitlin et al. 2013; Kerr 2013). In each solar

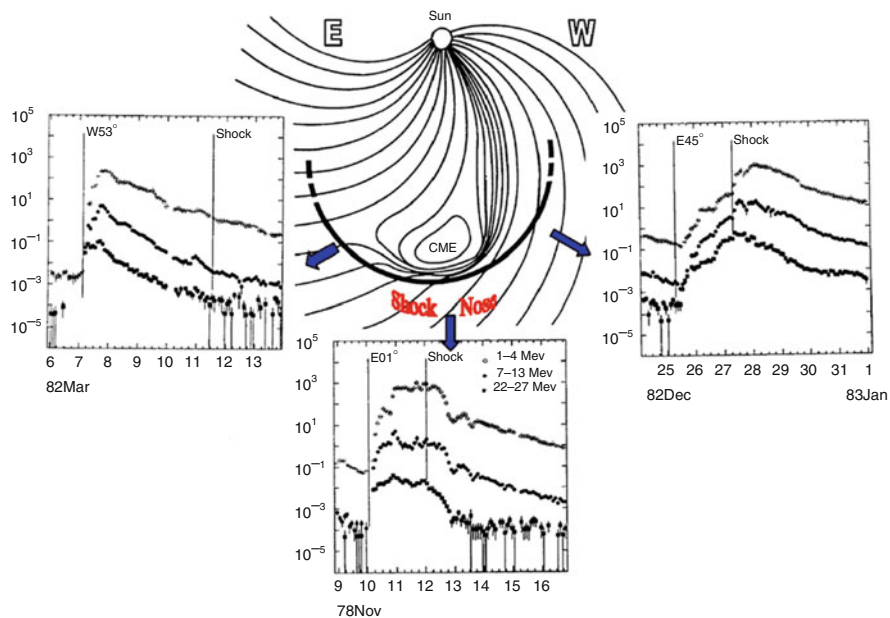


Fig. 1.4 Typical intensity–time profiles of 1–30 MeV protons for gradual SEP events observed at three different solar longitudes relative to the parent solar event. *Dashed lines* indicate the passage of shocks (Reproduced from Reames 2013, permission for reuse from publisher Springer for both print and electronic publication)

cycle several events of this intensity occur, thus, knowledge of the spectral knee energies is essential.

1.1.2 Large Gradual SEP Events

Early multi-spacecraft SEP observations revealed that 1–30 MeV proton time-intensity profiles in large gradual SEP events observed in the ecliptic plane at 1 AU are organized in terms of the longitude of the observer with respect to the traveling CME-driven shock and can be understood if the strongest acceleration occurs near the ‘nose’ of a CME-driven shock radially expanding outward from the Sun (see Fig. 1.4, Reames 2013; Cane et al. 1988; Cane and Lario 2006).¹ Figure 1.4 shows proton intensity profiles of several SEP events observed by the IMP-8 s/c as a function of longitude of the parent solar event. For observers at solar longitudes to the east of the source, the intensities have rapid rises peaking relatively earlier during the event when there is magnetic connection to the nose of the CME-shock

¹When observing images of the Sun east and west are reversed.

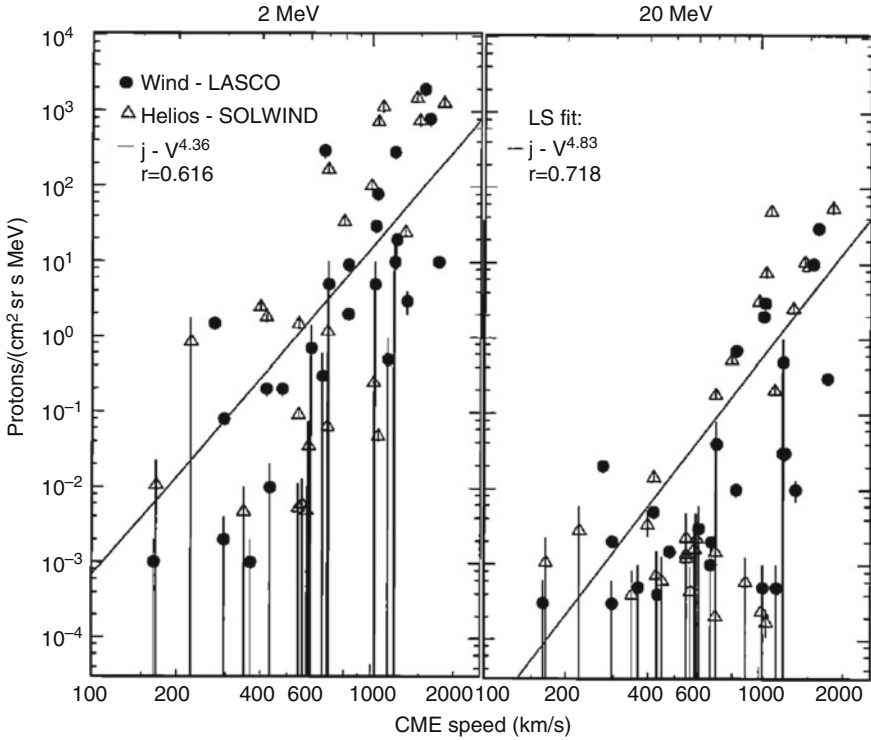


Fig. 1.5 Peak proton intensity in SEP events at 2 and 20 MeV as a function of CME speed. The different symbols denote two combinations of SEP instruments (Wind, Helios) and coronagraphs (LASCO, SOLWIND). Linear least-squares fits as well as the corresponding correlation coefficients are shown for each proton energy (Reproduced from Kahler 2001, permission for reuse from publisher John Wiley and Sons for both print and electronic publication)

near the Sun. Gradual decreasing intensities are observed subsequently, as the shock moves outward and the s/c becomes magnetically connected to the eastern flanks of the shock. For sources near the central meridian the proton intensities peak when the nose of the shock itself arrives at the s/c location. Observers located to the west of the source observe slowly rising intensities that peak after the local passage of the shock.

Comparison between the SEP and the CME or IP shock properties have shown no evidence of a clear correlation. In Fig. 1.5 (Kahler 2001) it is shown that CMEs with similar speeds are associated with a significant spread ($\sim 3\text{--}4$ orders of magnitude) in the peak proton intensities at 2 and 20 MeV of the associated SEPs at 1 AU. This study subsequently constituted the basis for comparison of a more recent multi-spacecraft study by (Rouillard et al. 2012) in which shock speeds could be measured where the shock intersected the field lines to each s/c in the heliosphere (see Sect. 1.1.4). Using a large number of SEP events, Kahler (2013a) examined the SEP-CME relationship calculating three different SEP event timescales: the onset time from CME launch to the 20 MeV SEP onset time, the rise time from

SEP onset to half the peak intensity and the duration of the SEP intensity above half the peak value. Comparison of these timescales with the CME properties such as speed, acceleration, width and location confirmed that faster (and wider) CMEs drive shocks, and accelerated SEPs over longer periods of time produce SEP events with longer timescales and larger fluences.

A flatter size distribution of SEP events relative to that of flare soft X-ray (SXR) events has been previously reported, with the power-law characterizing SEP size being significantly flatter than that of the SXR flux (e.g. Hudson 1978; Belov et al. 2007; Cliver et al. 2012). Cliver et al. (2012) have shown that this difference is primarily due to the fact that flares associated with large gradual SEP events are an energetic subset of all flares also characteristically accompanied by fast (>1000 km/s) CMEs that drive coronal/IP shock waves. They also concluded that the difference of ~ 0.15 between the slopes of the SEP event distributions and SEP SXR flares is consistent with the observed variation of SEP event peak flux with SXR peak flux. Kahler (2013b) presented arguments against using scaling laws for the description of the relationship between the size distributions of SXR flares and SEP events. They suggested an alternative explanation for flatter SEP power-law distributions in terms of the recent model of fractal-diffusive self-organized criticality proposed by Aschwanden (2012), providing evidence against a close physical connection of flares with SEP production. Trotter et al. (2015), although based on a limited SEP event sample, have recently studied the statistical relationships between SEP peak intensities of deka-MeV and near-relativistic electrons and characteristic parameters of CME and solar flares: the CME speed as well as the peak flux and fluence of SXR emission and the fluence of microwave emission. Via a partial correlation analysis they showed that the CME speed and SXR fluence are the only parameters that significantly affect the SEP intensity and concluded that both flare acceleration and CME shock acceleration contribute to the deka-MeV proton and near-relativistic electron populations in large SEP events.

Above a few tens of MeV per nucleon, large gradual SEP events are highly variable in their spectral characteristics and elemental composition. As an example, Fig. 1.6 (left) shows the event-integrated Fe/C ratio as a function of energy for the SEP events of April 21, 2002 and August 24, 2002 (Tylka et al. 2005). Both events were associated with flares nearly identical in terms of their sizes and solar locations ($\sim W80$), as well as with CMEs with similar speeds of ~ 2000 km/s, however, there were remarkable differences observed in their associated heavy ion spectral behaviour. To explain these differences, Cane et al. (2003) and Cane et al. (2006) proposed a direct flare particle component above ~ 10 MeV/nuc and that large SEP events are a mixture of flare-accelerated and shock-accelerated populations. According to this scenario, well-connected western hemisphere events are dominated by flare-accelerated particles above ~ 10 MeV/nuc, causing the significant increase of Fe/O, and could also account for the increasing energy dependence of the Fe/O ratios observed e.g. during the August 24, 2002 event. On the other hand the CME shock during the April 21, 2002 event is strong enough to accelerate >10 MeV/nucleon particles at 1 AU and lead to the observed Fe/O decrease with increasing energy.

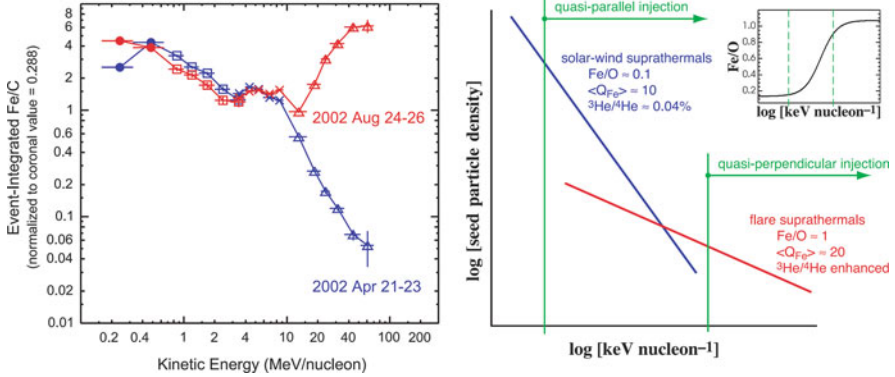


Fig. 1.6 The *left panel* shows a comparison of the energy dependence of the event-integrated Fe/C for the two SEP events of 21 April 2002 (*blue*) and 24 August 2002 (*red*) which are otherwise similar in their properties (Tylka et al. 2005). The *right panel* shows hypothetical spectra of the suprathermal seed populations for shock-accelerated SEPs, comprising both solar wind and flare-accelerated ions. Different injection thresholds will yield different abundance ratios (Reproduced from Reames 2013, permission for reuse from publisher Springer for both print and electronic publication)

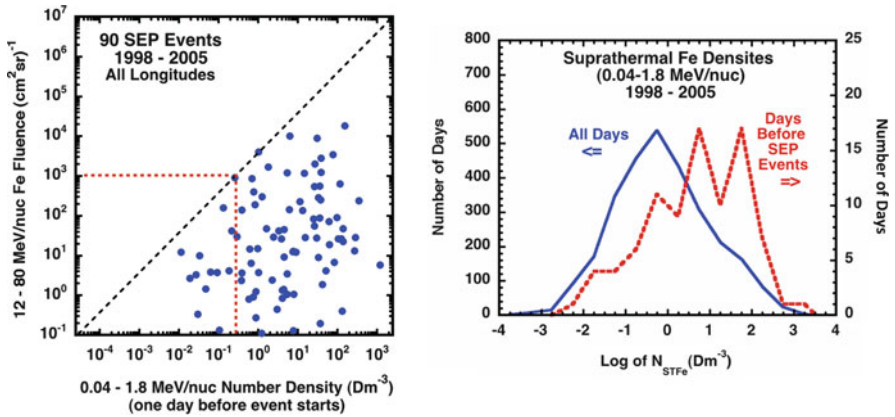


Fig. 1.7 (*left*) The 90 large SEP events defined as events with >12 MeV/nucleon Fe fluences > 0.1/(cm² sr) from 1998 to 2005. Days with high fluence only occur when the density of pre-existing suprathermal Fe was >0.3 Dm⁻³. (*right*) Histogram of daily averaged suprathermal Fe densities for all days from March 1998 to December 2005 (Reproduced from Mewaldt et al. 2012a, permission for reuse from publisher AIP Publishing LLC for both print and electronic publication)

Re-acceleration of remnant flare suprathermals or from accompanying flares has been another plausible idea to account for the observed elemental composition variability in SEP events. Mewaldt et al. (2012a) examined the dependence of SEP fluences on suprathermal seed-particle densities. In Fig. 1.7 (left) the Fe fluence in 90 large SEP events is compared with the pre-existing number density of suprathermal Fe at 1 AU 1 day before the occurrence of the SEP event. They

found that the maximum Fe daily-average SEP fluences measured by ACE/SIS are apparently limited by the pre-existing suprathermal number density. In Fig. 1.7 (right) it is shown that the suprathermal Fe densities are significantly greater before the occurrence of these large SEP events with respect to all other days, strongly suggesting that the large fluences of Fe in SEP events only occurred when there was a pre-existing high density of suprathermal Fe. According to these authors remnant flare suprathermal ions, as well as suprathermal material accelerated at previous CME shocks, existed in the heliosphere and served as seed particles subsequently re-accelerated by the CME shock that produced the large CME event (Mason et al. 1999; Desai et al. 2006).

An alternative scenario that (Tylka et al. 2005) proposed is that the observed variability in the energy dependence of the Fe/O ratio could be due to the interplay of two factors namely the evolution in the shock-normal angle as the shock moves outward from the Sun and a compound seed population, typically comprising at least suprathermals from the corona (or solar wind) and flare suprathermals. In this scenario, (Fig. 1.6, right), since the quasi-perpendicular (Q-Perp) shock needs higher injection energy, it may only effectively accelerate impulsive suprathermals originating from the flare acceleration process to high energy, producing the Fe-rich events. On the other hand, since quasi-parallel (Q-Par) shocks have lower injection thresholds they can accelerate the ambient solar wind (or coronal suprathermal ions) producing the Fe-poor events at higher energies. Tylka and Lee (2006) formalized the ideas put forward by Tylka et al. (2005) in an analytical model which above ~ 1 MeV/nucleon the Tylka and Lee (2006) model reproduced key features of the SEP variability observed in terms of the energy dependence of Fe/O, the $^3\text{He}/^4\text{He}$ ratio and the mean ionic charge state of Fe. Schwadron et al. (2015) further improved the model of coronal shock acceleration. In the left panel of Fig. 1.8, the injection energy of shock-accelerated particles is shown as a function of θ_{BN} for a range of the perpendicular to parallel diffusion coefficient ratios, whereas in the right panel, the time profiles of the shock or compression radial position (top panel) and θ_{BN} (bottom

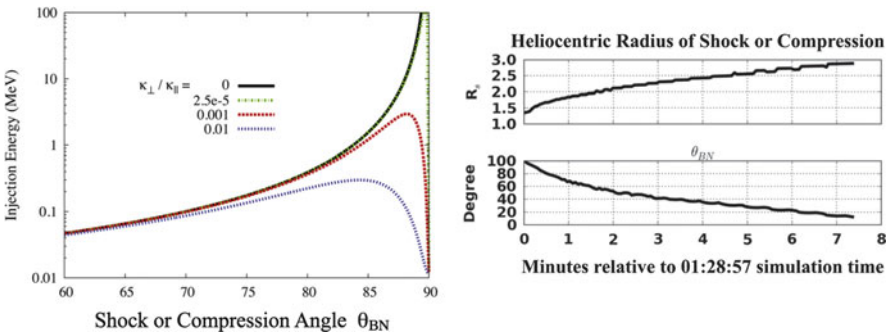


Fig. 1.8 *Left panel:* the injection energy of shock-accelerated particles as a function of θ_{BN} for a range of the perpendicular and parallel diffusion coefficient ratio. *Right panel:* Time profiles of the shock radial position θ_{BN} relative to 01:28:57 in the simulation time (see text) (© AAS. Reproduced with permission from Schwadron et al. 2015)

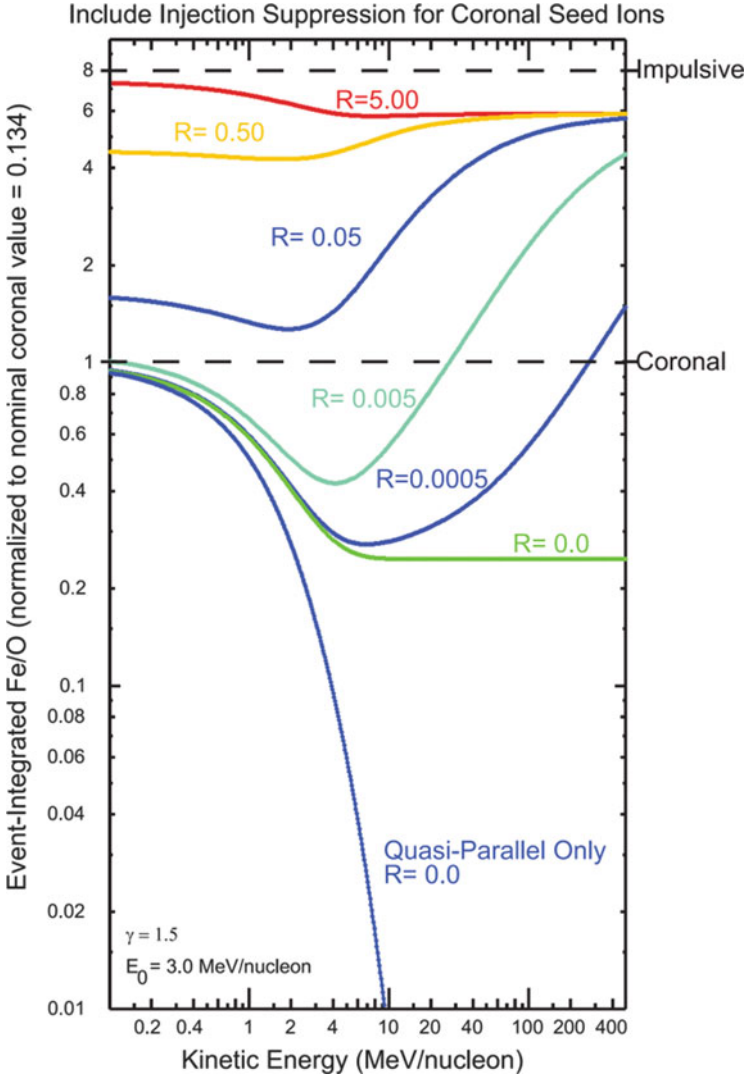


Fig. 1.9 Energy dependence of $(\text{Fe}/\text{O})_n$ predicted by the Tylka and Lee (2006) model shown for different values of the parameter R , which reflects the relative strengths of the remnant flare and coronal source contributions at a parallel shock, where seed ions from both populations are injected with equal efficiency (Reproduced from Reames 2013, permission for reuse from publisher Springer for both print and electronic publication)

panel) relative to 01:28:57 in the simulation time are shown. Apparently as the shock moves outward, θ_{Bn} decreases, and the geometry of the shock would change from Q-Perp to Q-Par. Schwadron et al. (2015) noted that the CME expansion and acceleration in the low corona may naturally give rise to rapid particle acceleration and broken power-law distributions in large SEP events. Figure 1.9 shows the results

of the (Tylka and Lee 2006) model for the case in which the injection of coronal seed ions at Q-Perp shocks is suppressed. The energy dependence of the normalized Fe/O ratio i.e. $(\text{Fe}/\text{O})_n$ is shown for different values of the impulsive suprathermal fraction R in the seed population. In the Q-Par shock event $(\text{Fe}/\text{O})_n \sim 1$ at lower energies ($E < 2$ MeV/nucleon), while $(\text{Fe}/\text{O})_n$ monotonically decreases with increasing E . In contrast, in the Q-Perp shock $(\text{Fe}/\text{O})_n$ is between 1 and 8 at lower energies, depending on the impulsive suprathermal fractions. With increasing energy the normalized ratio exhibits a complex variation e.g. approaching a plateau or reaching a minimum and further increasing afterwards. Tylka et al. (2005) hence assumed that the high-energy Fe/O ratio could be used as a crude proxy for shock geometry, with Fe-poor and Fe-rich events corresponding to Q-Par and Q-Perp shock geometries, respectively.

It should be noted that these explanations have not taken into account the IP transport effect, which could further distort the Fe/O ratio that emerged from the CME-shock acceleration process (e.g. Tylka et al. 2013). Recently, (Tan et al. 2017) examined 29 large SEP events with peak proton intensity $J_{pp} (>60 \text{ MeV}) > 1$ pfu during solar cycle 23. The emphasis of their examination was put on a joint analysis of the Ne/O and Fe/O data in the 3–40 MeV/nucleon energy range as covered by the Wind/LEMT and ACE/SIS sensors in order to differentiate between the Fe-poor and Fe-rich events at higher energies that emerged from the CME-driven shock acceleration process, after correcting the IP transport effect. One of the main findings of this work is presented in Fig. 1.10 in which the plot of the source plasma temperature T as very recently reported by Reames (2016) versus the normalized Ne/O ratio i.e. $(\text{Ne}/\text{O})_n$ at $E = 30$ MeV/nucleon is shown. T is well correlated with $(\text{Ne}/\text{O})_n$ with the linear correlation coefficient (CC) = 0.82. Therefore, the $(\text{Ne}/\text{O})_n$ value at high energies should be a proxy of the injection energy in the shock acceleration process, and hence the shock θ_{Bn} according to the models of Tylka and Lee (2006) and Schwadron et al. (2015).

1.1.3 Ground Level Enhancement (GLE) Events

Ground Level Enhancement (GLE) events form a particular case of high-energy SEP events associated with \sim GeV protons. These events pose severe radiation hazards to astronauts and technological assets in space and disrupt airline communications (Shea and Smart 2012). GLEs are nowadays measured with better coverage from space than at ground level, including ~ 80 MeV/amu to ~ 3 GeV/amu H and He spectra (Adriani et al. 2011), onsets (Reames 2009a, b), energy spectral shapes and abundances (Mewaldt et al. 2012b), electrons (Kahler 2007, 2012; Tan et al. 2013) and general properties (Gopalswamy et al. 2012). Rouillard et al. (2016) recently studied the link between an expanding coronal shock and the energetic particles measured near Earth during the GLE of 17 May 2012. The analysis showed that the GLE event occurred inside a clear magnetic cloud (see e.g. Malandraki et al. 2002). Using a new technique developed to triangulate the three-dimensional

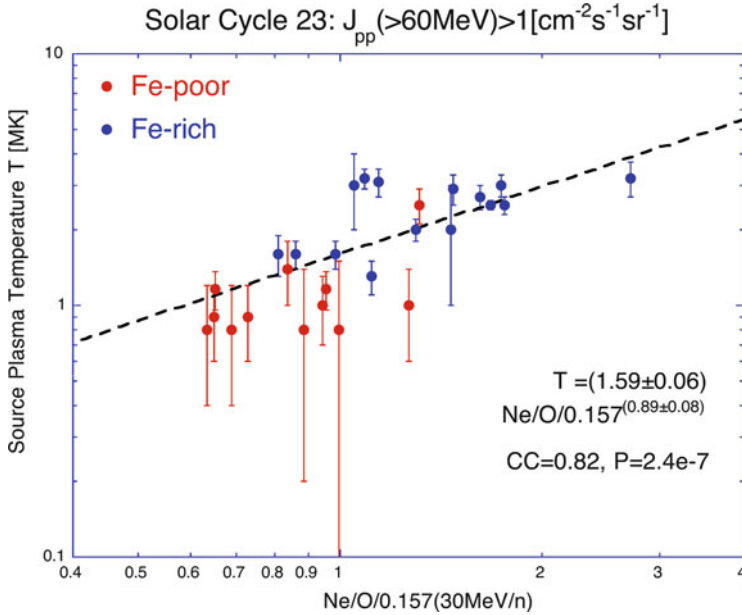


Fig. 1.10 Source plasma temperature T very recently reported by Reames (2016) is plotted vs. the $\text{Ne}/\text{O}/0.157$ (30 MeV/nucleon) value for the large Fe-poor (red) and Fe-rich (blue) events during solar cycle 23. The dashed line is the least-square fitting result for all the collected events as listed in Table 2 of Tan et al. (2017) (Reproduced from Tan et al. 2017)

(3D) expansion of the shock forming in the corona it was found that the highest Mach number (M_{FM}) values appear near the coronal neutral line within a few minutes of the CME onset. This neutral line is usually associated with the source of the heliospheric current sheet (HCS) and plasma sheet. It was shown that the release time of GeV particles occurs when the coronal shock becomes super-critical ($M_{\text{FM}} > 3$).

1.1.4 Multi-Spacecraft Observations of SEP Events

In this section the differences in the SEP event characteristics as observed from different vantage points in the heliosphere are discussed. Figure 1.11 shows as an example the 1 March 1979 SEP event observed by three different s/c. Helios 1 encounters the event near central meridian and observes a peak in the 3–6 MeV proton intensity near the shock passage time. The intensities at the other s/c, after reaching a peak, begin to track closely those seen at Helios 1 after they enter the so-called ‘reservoir’ region (see also McKibben 1972; Roelof et al. 1992) in which the intensities and energy spectra are nearly identical. These results indicate that only a small number of particles can leak out of the reservoir. Observations have provided strong evidence for the location of magnetic ‘barriers’ in space beyond 1 AU and

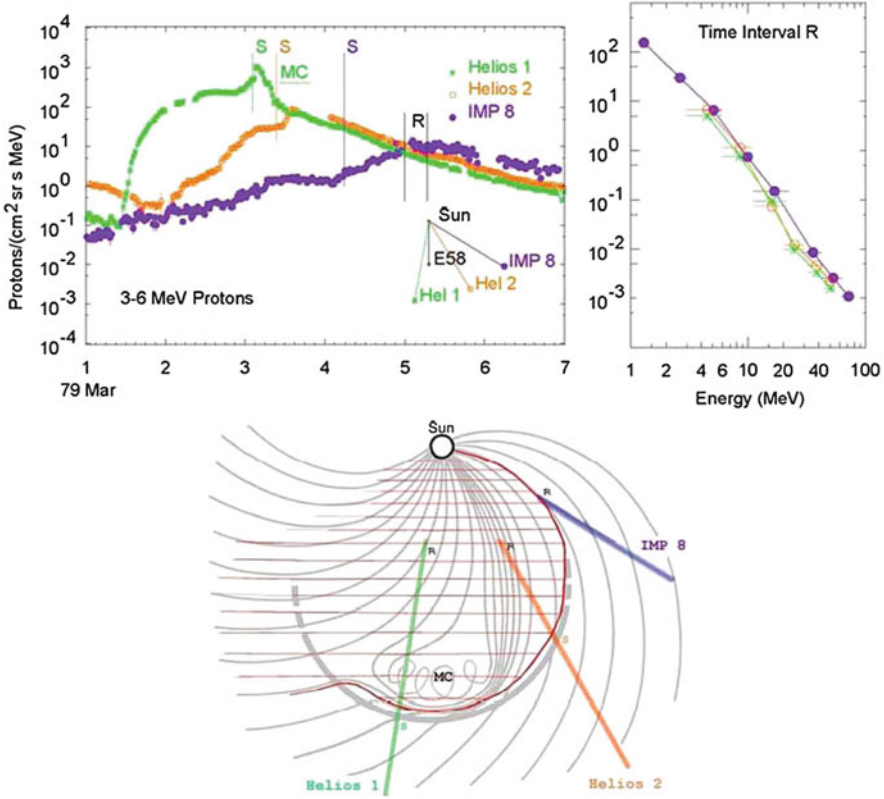


Fig. 1.11 The *top left panel* shows the intensity time-profiles for protons in the 1 March 1979 event at 3 s/c. ‘S’ denotes the time of shock passage at each s/c. The *top right panel* shows energy spectra in the ‘reservoir’ region behind the shock at time ‘R’. The *lower panel* shows the s/c trajectories through a sketch of the CME (Reproduced from Reames 2013, permission for reuse from publisher Springer for both print and electronic publication)

their role in determining the decay phase of SEP events and the establishment and maintenance of particle reservoirs in the heliosphere (Roelof et al. 1992, 2012a, b; Sarris and Malandraki 2003; Tan et al. 2012). Reames et al. (1996) also considered that the decay phase of the SEP events consists of particles propagating between the converging magnetic field near the Sun and a moving shell of strong scattering formed downstream of the distant traveling shocks. After formation, the reservoir slowly dissipates as a result of the nominal diffusion, convection, adiabatic cooling, and drift mechanisms that govern the propagation of SEPs.

The Ulysses European Space Agency (ESA)/National Aeronautics and Space Administration (NASA) mission provided unprecedented observations of the 3D heliosphere inside ~5 AU. Comparison of simultaneous SEP observations near the ecliptic plane with the Ulysses observations at high latitudes showed that most events that produce large high-energy (>20 MeV) proton and near-relativistic

electron flux increases near Earth also produce flux increases at high latitudes, regardless of the longitudinal, latitudinal and radial separation between the *s/c*, although with somewhat lower maximum intensities and slower rise at Ulysses (McKibben et al. 2003; Lario and Pick 2008; Malandraki et al. 2009). Particle anisotropies during SEP events at high latitudes are typically directed outward from the Sun and aligned with the local magnetic field (McKibben et al. 2003; Malandraki et al. 2009).

The observed field-aligned anisotropies, with components perpendicular to the local magnetic field that are essentially zero, indicate that there is no net flow of particles across the local magnetic field. The Ulysses observations revealed the 3D nature of the reservoir effects in the heliosphere. Dalla et al. (2003) concluded that the presence of a shock is not necessary for creating the near-equality observed at Ulysses and near Earth decay phases, but that these observations are better explained by diffusion across the interplanetary magnetic field (IMF).

More recently, combined observations by the twin STEREO *s/c* as well as near-Earth observatories revealed the wide longitudinal spreads of large gradual SEP events in the heliosphere and even strongly questioned the constraint of a narrow spread for ^3He -rich events (Wiedenbeck et al. 2013). A combination of physical processes appears to cause the large longitudinal spread of high-energy particles. Dresing et al. (2014) concluded that both an extended source region at the Sun and perpendicular transport in the IP medium are involved for most of the wide-spread events under study. The studies (Rouillard et al. 2011, 2012) found that the delayed SEP release times at STEREO and L1 are consistent with either the time required for the CME shock to reach field lines connected to the *s/c* or with the time required ($\sim 30\text{--}40$ min) for the CME to perturb the corona over a wide range of longitudes. Observations by Gómez-Herrero et al. (2015) indicated that higher SEP fluxes, harder SEP spectra and direct injections of SEPs onto well-connected IMF lines are associated with lateral expansions of CME-driven shocks in the low corona, and may therefore be responsible for the rapid longitudinal spread as observed at vastly distributed *s/c* in many SEP events. Other factors that may also play a role in distributing SEP events longitudinally include the large-scale IMF configuration inside interplanetary CMEs (ICMEs) (e.g. Kahler and Vourlidis 2013) and the relative strength of the CME shock, which depends on the local Alfvén speed, rather than the actual speed of the CME (e.g. Gopalswamy et al. 2014).

1.1.5 Particle Acceleration

Recently, important progress has occurred, both from the theoretical and the observational perspective in the research of small-scale magnetic islands in the solar wind and their role in particle acceleration. Khabarova et al. (2015) presented observations that show the occurrence of small-scale magnetic islands and related plasma energization in the vicinity of the HCS. They found evidence that magnetic islands experience dynamical merging in the solar wind and that increases of

energetic particle fluxes in the keV–MeV range are found to coincide with the presence of magnetic islands confined by strong current sheets (CSs). Moreover, the interaction of ICMEs with the HCS can lead to significant particle acceleration due to plasma confinement. Their observations confirmed the rippled structure of the HCS and since such a structure confines plasma, it makes possible the strong energization of particles trapped inside small-scale magnetic islands. They concluded that although initial particle acceleration due to magnetic reconnection at the HCS may be insufficient to obtain high energies, the presence of magnetic islands inside the ripples of the HCS or between two CSs with a strong guide field offers the possibility of re-accelerating particles in the ways discussed theoretically by Zank et al. (2014) and le Roux et al. (2015a).

Khabarova et al. (2016) further explored the role of the heliospheric magnetic field configurations and conditions that favor the generation and confinement of small-scale magnetic islands associated with the so-called atypical energetic particle events (AEPEs) in the solar wind. Some AEPEs have been found not to align with standard particle acceleration mechanisms, such as flare-related or simple diffusive shock acceleration processes related to ICMEs and corotating interaction regions (CIRs). They provided more observations fully supporting the idea and the theory of particle energization by small-scale-flux-rope dynamics previously developed by Zank et al. (2014, 2015a, b) and le Roux et al. (2015a, b). If the particles are pre-accelerated to keV energies via classical mechanisms, they may be additionally accelerated up to 1–1.5 MeV inside magnetically confined cavities of various origins. Khabarova et al. (2016) showed that particle acceleration inside magnetic cavities may explain puzzling AEPEs occurring far beyond IP shocks, within ICMEs, before approaching CIRs, as well as between CIRs. SEP transport processes are described in detail in Chap. 4 of this volume (see also Desai and Giacalone (2016) which includes a review on this topic).

1.1.6 Key Open Questions and Future Missions

Solar Orbiter (SoLO) is a unique ESA/NASA joint mission conceived to unveil the Sun-heliosphere connection (Mueller et al. 2013), expected to be launched in 2019. The orbital configuration includes a close perihelion, high inclination intervals allowing the observation of the solar polar regions and quasi-co-rotation periods. One of the top-level science questions is “How do solar eruptions produce energetic particle radiation that fills the heliosphere?” which can be broken down into three inter-related key topics: What are the seed populations for energetic particles? How and where are energetic particles accelerated at the Sun? How are energetic particles released from their sources and distributed in space and time?

The Energetic Particle Detector (EPD) instrument suite onboard SoLO (Principal Investigator: Prof. J. Rodríguez-Pacheco, Spain) will measure energetic electrons, protons and ions, operating at partly overlapping energy ranges covering from a few keV to 450 MeV/nucleon. The EPD sensors will measure the composition, spectra

and anisotropies of energetic particles with sufficient temporal, spectral, angular and mass resolution to achieve the mission goals (Gómez-Herrero et al. 2016). Energetic particles escaping from the acceleration sites propagate through the turbulent IMF. Previous observations by the Helios *s/c* have shown that SEP events near the Sun are much less affected by IP transport effects compared to 1 AU observations. As the *s/c* moves further away from the Sun, scattering and diffusion processes become more important and multiple injections closely spaced in time cannot be resolved (Wibberenz and Cane 2006). Thus, SolO observations close to the perihelion will be crucial to unveil SEP injection, acceleration, release and transport processes, in view of the ongoing debate about the SEP acceleration sites, disentangling the acceleration at CME-driven shocks and at reconnection sites in solar flares (e.g. Malandraki et al. 2006).

NASA's Solar Probe Plus mission, recently re-named to Parker Solar Probe to honour pioneering physicist Prof. Eugene Parker, will fly within nine solar radii of the Sun's surface and is scheduled to be launched in July 2018. The two Energetic Particle Instruments (EPI) of the Integrated Science Investigation of the Sun (ISIS) (Principal Investigator: Prof. D. J. McComas, USA) will measure lower (EPI-Lo) and higher (EPI-Hi) energy particles. EPI-Lo will measure ions and ion composition from ~ 20 keV/nucleon–15 MeV total energy and electrons from ~ 25 –1000 keV. EPI-Hi measures ions from ~ 1 –200 MeV/nucleon and electrons from ~ 0.5 –6 MeV. The unique ISIS observations will allow the exploration of the mechanisms of energetic particles dynamics, including their (1) Origin: defining the seed populations and physical conditions necessary for energetic particle acceleration; (2) Acceleration: determining the role of shocks, reconnection, waves and turbulence in accelerating energetic particles; (3) Transport: revealing how energetic particles propagate from the corona out into the heliosphere (McComas et al. 2016).

It is evident that the next decade is expected to revolutionize our understanding of SEP acceleration and transport, by means of state-of-the-art sensors on board these two upcoming missions providing unique and unprecedented measurements for the exploration of the solar corona and inner heliosphere. Synergies between the two missions are of particular relevance, since both missions have overlapping timelines and the Parker Solar Probe perihelion, reaching up to ~ 9 solar radii, will permit simultaneous in-situ observations at the SEP acceleration region close to the Sun and at larger radial distances, with continuous remote sensing coverage provided by SolO and near-Earth *s/c*. Radial alignments between the two *s/c* will enable the observations of plasma 'entities' from the same solar source region at progressive radial distances as well as the study of energetic particle radial gradients. Furthermore, other useful configurations for the optimization of the science return are alignments along the same IMF line allowing the observation of SEPs originating at the same acceleration site by two or more *s/c* located at different radial distances. SEP event observations by multiple *s/c* located at widely separated points in the heliosphere, both in longitude and in latitude, will be valuable for the investigation of the spatial distribution of SEPs and the unraveling of the physical

mechanisms responsible for producing wide-spread SEP events (see e.g. Sect. 1.1.4) (Gómez-Herrero et al. 2016).

1.2 Applications

1.2.1 Why Study SEP Events?

It has become apparent during the last decades that SEP events pose important challenges for modern society. Due to their unpredictability, specifically for those that reach relativistic velocities (high energies) and peak values in very short time scales, they are of concern. SEPs ranging from protons to heavy ions up to iron have been found to have impacts on space systems (s/c, instruments, electronic components, solar arrays, . . .), avionics and living organisms (e.g. Feynman and Gabriel 2000; Jiggins et al. 2014). It has even been suggested that systems with very high safety and reliability requirements (e.g. in the nuclear power industry) may need to take account of superstorm ground level radiation on microelectronic devices within the system.

In the case of nuclear power a Carrington event may not be a sufficient case since relevant timescales for risk assessment may be as long as 10,000 years.

(Paul Cannon (Cannon et al. 2013))

In the following some of the most important and common SEP induced effects are presented, as well as mitigation strategies currently being relied on.

1.2.2 SEP Effects on Technology

Developments in technology such as miniaturization has no doubt benefited space industry, but at the same time technical equipment has increasingly become more vulnerable to the space environment. On a lesser scale the well-known “snow” effect, resulting from the increase in high energy protons during intense SEP events is sometimes seen on coronagraphic images, as shown in Fig. 1.12, obscuring the image of the CME itself. However, in some instances SEP induced effects may be of such a nature that they can result in long-term damage. Missions that target the inner solar system are especially vulnerable to high-energy charged particles (DiGregorio 2008).

Table 1.1 presents a summary of SEP induced effects observed onboard s/c and aircraft. It is clearly shown how both the energy and species of the particles being considered is an important factor for evaluating their potential effect. Particle flux intensities at lower energies are important for effects such as solar cell degradation, whereas nuclear interactions are associated with particle flux intensities at higher

Fig. 1.12 The snowstorm effect observed on the LASCO/SoHO coronagraph on 28 Oct. 2003. Image: ESA/NASA—SOHO/LASCO

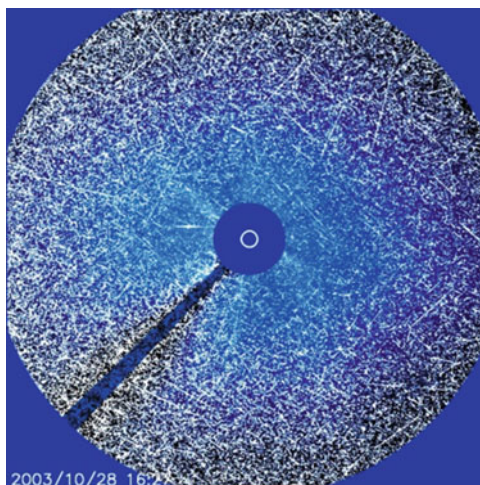


Table 1.1 Particle effects on technology observed as a function of the particle energy range

Energy range	Effects
Protons <10 MeV	Material and solar cell effects over time as a result of cumulated dose (e.g. solar cell degradation)
Protons >10 MeV	Nuclear interactions (e.g., sensor background noise, ionization, displacement damage)
Protons >50 MeV and Ions >10 MeV nucleon ⁻¹	Nuclear interactions (e.g., single event effects in electronics onboard satellites, as well as aircraft)

energies. Single-event effects (SEEs) are classified as either non-destructive or destructive:

- **Single Event Upsets:** Occurs in logical circuits and is defined as a bit switching from an initial logical state to an opposite logical state.
- **Single Event Latchup:** Results in a high operating current, above device specifications, and must be cleared by a power reset.
- **Single Event Gate Rupture:** Occurs in powerful transistors and is manifested by an increase in gate leakage current
- **Single Event Burnout:** A condition that can cause device destruction due to a high current state in a power transistor.

For s/c mission planning and operations SEP events are considered. In regard to launch operations the SEP environment is also a decisive factor whether to give the go ahead to launch or not for several reasons. Launch vehicles and s/c reaching sufficiently high geomagnetic latitudes could for example see an increase in SEE rates at times of significant SEP events. On the other hand, optical instruments are also vulnerable to SEPs and induced sensor interference can disrupt the operation of star trackers and put critical s/c manoeuvres at risk.

Under normal space weather conditions Earth's magnetosphere acts as a shield and protects us from charged particles and magnetic clouds. Nevertheless at times SEPs may have sufficient energies to "break" through this shield and enter the ionosphere; SEPs have easier access to the polar regions near Earth's magnetic poles than at the equator due to the "open" magnetic field lines. The cutoff latitude is a function of a particle's momentum per unit charge and is referred to as its rigidity (see Chap. 5). Variations in SEP access to latitudes can occur on time scales of an hour or less in response to changes in the solar wind dynamic pressure and IMF (Kress et al. 2010). For this reason high inclination LEO satellites can at times be vulnerable to SEPs, as well as the International Space Station that has an orbital inclination of 51.64° .

SEP events can also effect signal propagation between Earth and satellites. Polar cap absorption (PCA) events result from intense ionisation of the D-layer of the polar ionosphere by strong (>10 MeV) SEP events. Due mainly to protons with energy in the range of 1–100 MeV (corresponds to an altitude between 30 and 80 km) the increased ionisation absorbs radio waves in the HF and VHF bands, resulting in problems for communications (degraded radio propagation through the polar regions) and navigation position errors with the importance being a function of the individual SEP event.

Despite the relative steepness of SEP energy spectra, the small percentage of protons accelerating up to high energies (>500 MeV) still pose considerable problems. These high-energy SEP events such as the September 1989 SEP event (Fig. 1.3) are often associated with GLE events and can result in secondary radiation caused by particles interacting with s/c shielding and other material. This results in the production of particles such as lower energetic protons, neutrons, and pions that in some cases may be more of an obstacle for the s/c designer than the primary SEPs themselves. While the former can induce SEEs, secondary particle background can have more profound effects on sensitive space-borne instrumentation.

Technology onboard commercial airline operations can also be affected by SEP events including avionics (electronic systems), communications and GPS navigation systems (Jones et al. 2005). Specifically ultra-long-haul "over-the-pole" routes and high-latitude flights are susceptible to these SEP induced effects.

1.2.3 SEPs and Human Health Effects

In addition to being a threat to technology, SEP events are also an important risk to human health. Since the Apollo missions to Earth's Moon in the 1970s human space exploration has mainly been focused on low-Earth orbit altitudes (e.g. Space Shuttle, International Space Station) and suborbital flights. Outside Earth's magnetosphere SEP events have for the most part been a concern for robotic flight missions up until now. During the last decades the vision for space exploration has changed as space agencies and private companies are contemplating sending humans to Mars and asteroids, and as the population on Earth increases colonizing such targets and pursuing deep space exploration will only become more and more attractive. The

downside is that human interplanetary exploration will expose astronauts not only to the galactic cosmic ray background but at times also to increased levels of radiation during SEP events and this may indeed be the most important obstacle to overcome.

The field of radiation biology concerns how the radiation environment of space affects cells. Radiation effects on astronauts are sub-classed into two categories:

1. Deterministic (early) Effects: Due to exposure to a large dose of radiation for a limited time (ranges from hair loss, nausea, acute sickness, death)
2. Stochastic (late) Effects: Due to random radiation-induced changes at the deoxyribonucleic acid (DNA) molecule level (cancer).

As already mentioned in Sect. 1.1.1 protons with high energies (>30 MeV) are a health risk for astronauts. For this reason protons with energies >10 MeV are continuously monitored and taken into account when planning extra-vehicular activities.

In those instances SEP events reach aviation altitudes they become also a concern for human health as the radiation dose received can increase. This specifically applies to high-latitude flights ($>50^\circ\text{N}$) and polar routes ($>78^\circ\text{N}$). For commercial aviation this can be a risk for frequent flyers and particularly for aircrew. Effective pilot training programs as well as monitoring, measuring, and regulatory measures in regard to radiation exposure risks for both human tissue and avionics are recognized by a broad community (Tobiska et al. 2015).

1.2.4 Mitigating the Effects of SEPs

The SEP radiation environment is assessed when designing s/c, for s/c mission planning and operations, and when human spaceflight is involved. How does one best go about protecting assets in space and on the ground from the effects of SEP events? For this purpose post-event analysis “hazard assessment” is performed after an anomaly occurs (is recorded). Furthermore, mitigation procedures are put in place before launch (e.g. s/c shielding, redundancy onboard) and during operations SEP forecasting takes place.

1.2.4.1 Hazard Assessment

Analyzing s/c anomalies (hazard assessment) is one way to infer whether an observed anomaly was due to technical or human error, or whether it was a direct consequence of space environment conditions. In Fig. 1.13 it is clearly seen that there was an increase in the number of SEUs in the Ramdisk onboard the LEO Algerian Alsat-1 satellite during three SEP events (29/10/2003: 790 SEUs, 20/01/2005: 774 SEUs, 13/12/2006: 303 SEUs). Figure 1.14 illustrates that the SEU rate is directly a function of the SEP energy spectrum; the flatter the spectrum the higher the number of SEUs (Bentoutou and Bensikaddour 2015).

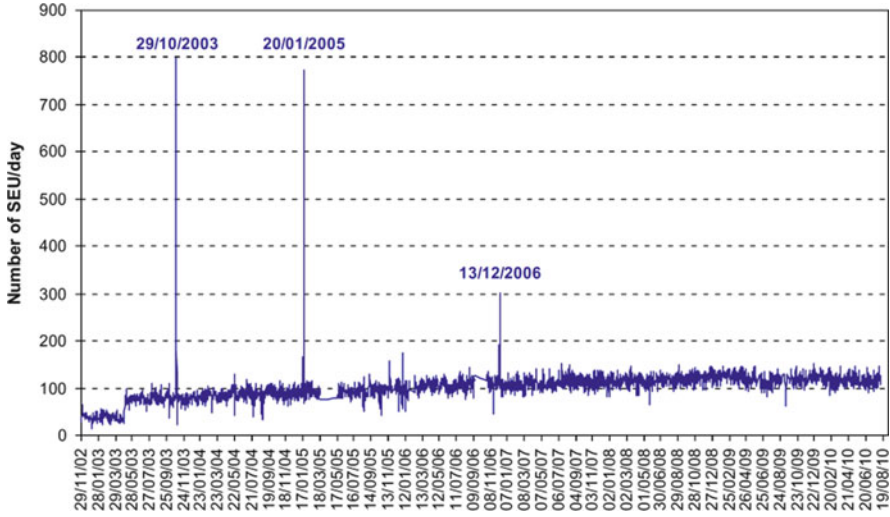


Fig. 1.13 The daily SEU rate observed on the Alsat-1 Ramdisk during the previous solar cycle (Reproduced from Bentoutou and Bensikaddour 2015, permission for reuse from publisher Elsevier for both print and electronic publication)

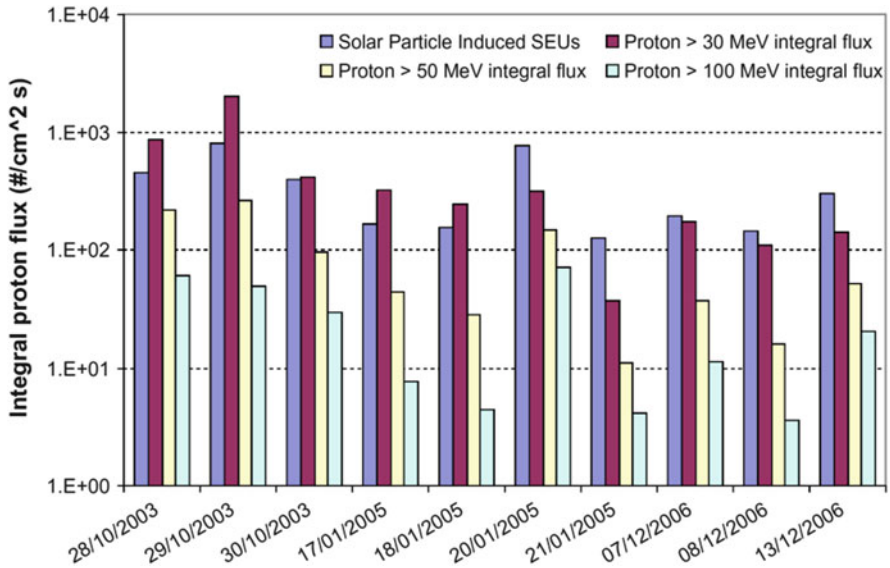


Fig. 1.14 SEU rate (purple bars) with proton energy spectrum composition (>30 MeV, >50 MeV, >100 MeV integral flux) when significant SEP events were observed (28–30/10/2003, 17–18/01/2005, 20–21/01/2005, 7–8/12/2006, 13/12/2006) (Reproduced from Bentoutou and Bensikaddour 2015, permission for reuse from publisher Elsevier for both print and electronic publication)

Information obtained from hazard assessment can provide useful input for both engineering (mitigation) and scientific approaches (forecasting), and establish a one-to-one correction between space environment conditions and technical failures. However, *s/c* operators are sometimes reluctant in providing anomaly data due to confidentiality issues specifically when the anomaly is an important one (e.g. loss of *s/c*); this makes it sometimes difficult to assess whether a failure was due to the space environment or not. To complement hazard assessment one therefore relies on efficient mitigation strategies such as *s/c* shielding and forecasting techniques.

1.2.4.2 Mitigation Procedures

The classical engineering approach is based on passive shielding that can protect the crew and hardware (exterior and interior) of the *s/c* and understanding how the space environment interacts with the shielding. For this reason SEP energy spectra are used as input in engineering tools when computing induced effects such as the dose encountered on technology and humans during SEP events. The shape of the spectrum is important as worst-case scenarios are application dependent, meaning that the flux intensity at lower energies are important for material and solar cell effects. At the other end of the energy spectrum, flux intensities at higher energies are more important for nuclear interactions (e.g., background noise, single event upsets).

Aluminium is generally the material used when building most *s/c* shielding structures and this type of shielding protects against SEP proton events for the most part (Wilson et al. 1997). However, the higher the particle energy, for example in the case of extreme events, the thicker the shielding material necessary to stop the primary particles. This not only implies the possibility of secondary radiation but also higher costs. For these reasons SEP event forecasting is also relied upon to mitigate against SEP events. Currently, short-term SEP event forecasting systems are based on:

- theoretical understanding (e.g. physical models),
- remote sensing of phenomena such as solar flares, CMEs and active regions
- space-based in-situ observations at L1 (shock arrival, energetic storm particles) and GEO
- historical data
- ground-based observations (e.g. radio, neutron monitors).

and can roughly be divided in two categories:

- (a) Physics-based numerical models (e.g. Earth-Moon-Mars Radiation Environment Module (EMMREM) (Schwadron 2010), Predictions of radiation from REleASE, EMMREM and Data Incorporating CRaTER, COSTEP and other SEP measurements (PREDICCS) (Schwadron 2012), Solar Energetic Particle MODEL (SEPMOD) (Luhmann et al. 2010), SOLar Particle ENgineering Code (SOLPENCO) (Aran et al. 2006), and SOLPENCO2 (provides SEP modelling

away from 1 AU to the SEP statistical model of the SEPTEM project (Crosby et al. 2015)))

- (b) Empirical models (e.g. University of Malaga Solar Energetic Particle (UMASEP) system (Núñez 2011), Relativistic Electron Alert System for Exploration (REleASE) (Posner 2007), Proton Prediction System (PPS) (Kahler et al. 2007), PROTONS system (Balch 2008), GLE Alert Plus (Kuwabara et al. 2006; Souvatzoglou et al. 2014) and Laurenza’s approach (Laurenza et al. 2009))

In some cases forecasting systems rely on methods from both categories such as the SEPForecast tool built under the EU FP7 COMESEP project (263252) (Crosby et al. 2012), (<http://www.comesep.eu/alert/>).

The EU H2020 HESPERIA project (637324) developed two novel real-time SEP forecasting tools based on the UMASEP and REleASE proven concepts:

- The HESPERIA UMASEP-500 tool makes real-time predictions of the occurrence of GLE events, from the analysis of SXR and differential proton flux measured by the GOES satellite network.
- The HESPERIA REleASE tool generates expected proton flux alerts at two energy ranges (15.8–39.8 MeV and 28.2–50.1 MeV) making use of relativistic electrons ($v > 0.9 c$) provided by the Electron Proton Helium Instrument (EPHIN) on SOHO and near-relativistic ($v < 0.8 c$) electron measurements from the Electron Proton Alpha Monitor (EPAM) aboard the Advanced Composition Explorer (ACE).

Both of these new tools are operational through the project’s website (<https://www.hesperia.astro.noa.gr/>) and described in detail in Chap. 7 of this volume.

Acknowledgements Olga E. Malandraki has been partly supported by the International Space Science Institute (ISSI) in the framework of International Team 504 entitled “Current Sheets, Turbulence, Structures and Particle Acceleration in the Heliosphere”.

References

- Adriani, O., et al.: *Astrophys. J.* **742**(2), 102 (2011)
- Aran, A.B., et al.: *Adv. Space Res.* **37**, 1240 (2006)
- Aschwanden, M.J.: *Astron. Astrophys.* **539**, A2 (2012)
- Balch, C.C.: *Space Weather.* **6**, S01001 (2008)
- Belov, A., et al.: *Solar Phys.* **246**(2), 457 (2007)
- Bentoutou, Y., Bensikaddour, E.-H.: *Adv. Space Sci.* **55**, 2820 (2015)
- Cane, H.V., Lario, D.: *Space Sci. Rev.* **123**(1), 45 (2006)
- Cane, H.V., et al.: *J. Geophys. Res.* **93**(A9), 9555 (1988)
- Cane, H.V., et al.: *Geophys. Res. Lett.* **30**, 8017 (2003)
- Cane, H.V., et al.: *J. Geophys. Res.* **111**(A10), A06S90 (2006)
- Cannon, P., et al. (eds.): *Extreme space weather: impacts on engineered systems and infra-structure.* Royal Academy of Engineering, London (2013)

- Cliver, E.W.: CP528: acceleration and transport of energetic particles observed in the heliosphere. In: Mewaldt, R.A., et al. (eds.) ACE 2000 Symposium, California, January 2000. AIP Conf. Proc., vol. 528, p. 21. AIP, New York (2000)
- Cliver, E.W., et al.: *Astrophys. J. Lett.* **756**, L29 (2012)
- Crosby, N.B., et al.: AIAC '11: space weather: the space radiation environment. Hu, Q., et al. (eds.) 11th Annual International Astrophysics Conference, PalmSprings, USA, March 2012. AIP Conf. Proc., vol. 1500, p. 159. AIP, New York (2012)
- Crosby, N., et al.: *Space Weather*. **13**, 406 (2015)
- Cucinotta, F.A., et al.: *Space Weather*. **8**(12), S00E09 (2010)
- Dalla, S., et al.: *Geophys. Res. Lett.* **30**(1), 8035 (2003)
- Desai, M.I., Giacalone, J.: *J. Living Rev. Sol. Phys.* **13**, 3 (2016)
- Desai, M.I., et al.: *Astrophys. J.* **649**(1), 470 (2006)
- DiGregorio, B.E.: *Space Weather*. **6**, 3 (2008)
- Dresing, N., et al.: *Astron Astrophys.* **567**, A27 (2014)
- Feynman, J., Gabriel, S.B.: *J. Geophys. Res.* **105**(A5), 10543 (2000)
- Forbush, S.E.: *Phys. Rev.* **70**, 771 (1946)
- Gómez-Herrero, R., et al.: *Astrophys. J.* **799**, 55 (2015)
- Gómez-Herrero, R., et al.: XXV European Cosmic Ray Symposium, Turin, 4–9 September (2016)
- Gopalswamy, N., et al.: *Astrophys. J. Lett.* **572**(1), L103 (2002)
- Gopalswamy, N., et al.: *Space Sci. Rev.* **171**(1), 23 (2012)
- Gopalswamy, N., et al.: *Earth Planets Space*. **66**, 104 (2014)
- Gosling, J.T.: *J. Geophys. Res.* **98**, 18937 (1993)
- Hudson, H.S.: *Solar Phys.* **57**, 237 (1978)
- Jiggins, P., et al.: *J. Space Weather Space Clim.* **4**, A20 (2014)
- Jones, J.B.L., et al.: *Adv. Space Res.* **36**, 2258 (2005)
- Kahler, S.W.: *J. Geophys. Res.* **106**, 20947 (2001)
- Kahler, S.W.: *Space Sci. Rev.* **129**, 359 (2007)
- Kahler, S.W.: *Astrophys. J.* **769**, 110 (2013a)
- Kahler, S.W.: *Astrophys. J.* **769**, 35 (2013b)
- Kahler, S.W., Vourlidis, A.: *Astrophys. J.* **769**, 143 (2013)
- Kahler, S.W., et al.: *JASTP*. **69**, 43 (2007)
- Kahler, S.W., et al.: *Space Sci. Rev.* **171**, 121 (2012)
- Kallenrode, M.B.: *J. Phys. G: Nucl. Part. Phys.* **29**, 965 (2003)
- Kerr, R.A.: *Science*. **340**(6136), 1031 (2013)
- Khabarova, O., et al.: *Astrophys. J.* **808**, 181 (2015)
- Khabarova, O., et al.: *Astrophys. J.* **827**, 122 (2016)
- Kress, B.T., et al.: *Space Weather*. **8**, 5 (2010)
- Kuwabara, T., et al.: *Space Weather*. **4**, S10001 (2006)
- Lario, D., Pick, M.: In: Balogh, A., et al. (eds.) *The heliosphere through the solar activity cycle*, p. 151. Springer/Praxis Publishing Ltd, Chichester (2008)
- Laurenza, M.E., et al.: *Space Weather*. **7**, 4 (2009)
- le Roux, J.A., et al.: *Astrophys. J.* **801**, 112 (2015a)
- le Roux, J.A., et al.: AIAC '14: Linear and nonlinear particle energization throughout the heliosphere and beyond. In: Zank, G.P. (eds.) 14th Annual International Astrophysics Conference, Florida, April 2015. *J. Phys.: Conc. Ser.*, vol. 642, p. 012015. IOP Publishing, USA (2015b)
- Lovell, J.L., et al.: *J. Geophys. Res.* **103**, 23733 (1998)
- Luhmann, J.G., et al.: *Adv. Space Res.* **46**, 1 (2010)
- Malandraki, O.E., et al.: *JASTP*. **64**(5–6), 517 (2002)
- Malandraki, O.E., et al.: Proceedings of the second solar orbiter workshop, Athens, 16–20 October 2006. ESA Publication (2006)
- Malandraki, O.E., et al.: *Astrophys. J.* **704**, 469 (2009)
- Mason, G.M., et al.: *Astrophys. J. Lett.* **525**, L133 (1999)
- McComas, D.J., et al.: *Space Sci. Rev.* **204**, 187 (2016)
- McKibben, R.B.: *J. Geophys. Res.* **77**(2), 3957 (1972)

- McKibben, R.B., et al.: *Ann. Geophys.* **21**(6), 1217 (2003)
- Mewaldt, R.A., et al.: AIAC '11: Space weather: the space radiation environment. Hu, Q. et al. (eds.) 11th Annual International Astrophysics Conference, PalmSprings, USA, March 2012. AIP Conf. Proc., vol. 1500, p. 128. AIP, New York (2012a)
- Mewaldt, R.A., et al.: *Space Sci. Rev.* **171**, 97 (2012b)
- Meyer, P., et al.: *Phys. Rev.* **104**, 768 (1956)
- Mueller, D., et al.: *Solar Phys.* **285**, 25 (2013)
- National Research Council (NCR): Managing space radiation risk in the new era of space exploration. The National Academies Press, Washington, DC (2008)
- Núñez, M.: *Space Weather.* **9**, S07003 (2011)
- Posner, A.: *Space Weather.* **5**, S05001 (2007)
- Reames, D.V.: *Space Sci. Rev.* **90**, 413 (1999)
- Reames, D.V.: *Astrophys. J.* **693**, 812 (2009a)
- Reames, D.V.: *Astrophys. J.* **706**, 844 (2009b)
- Reames, D.V.: *Space Sci. Rev.* **175**, 53 (2013)
- Reames, D.V.: *Sol. Phys.* **291**(3), 911 (2016)
- Reames, D.V., et al.: *Astrophys. J.* **466**, 473 (1996)
- Roelof, E.C.: AIAC '11: Space weather: the space radiation environment. In: Hu, Q., et al. (eds.) 11th Annual International Astrophysics Conference, PalmSprings, USA, March 2012. AIP Conf. Proc., vol. 1500, p. 174. AIP, New York (2012a)
- Roelof, E.C.: AIAC '11: Space weather: the space radiation environment. In: Hu, Q., et al. 11th Annual International Astrophysics Conference, PalmSprings, USA, March 2012. AIP Conf. Proc., vol. 1500, p. 180. AIP, New York (2012b)
- Roelof, E.C., et al.: *Geophys. Res. Lett.* **19**, 1243 (1992)
- Rouillard, A., et al.: *Astrophys. J.* **735**, 7 (2011)
- Rouillard, A.P., et al.: *Astrophys. J.* **752**, 44 (2012)
- Rouillard, A.P., et al.: *Astrophys. J.* **833**, 45 (2016)
- Sarris, E.T., Malandraki, O.E.: *Geophys. Res. Lett.* **30**(21), 2079 (2003)
- Schwadron, N.A.: *Space Weather.* **8**, 1 (2010)
- Schwadron, N.A.: *Space Weather.* **10**, 10 (2012)
- Schwadron, N.A., et al.: *Astrophys. J.* **810**(2), 97 (2015)
- Shea, M.A., Smart, D.F.: *Space Sci. Rev.* **171**, 161 (2012)
- Souvatoglou, G., et al.: *Space Weather.* **12**, 11 (2014)
- Tan, L.C., et al.: *Astrophys. J.* **750**, 146 (2012)
- Tan, L.C., et al.: *Astrophys. J.* **768**, 68 (2013)
- Tan, L.C., et al.: *Astrophys. J.* **835**(2), 192 (2017)
- Tobiska, W.K., et al.: *Space Weather.* **13**, 4 (2015)
- Trottet, G., et al.: *Solar Phys.* **290**, 819 (2015)
- Tylka, A.J., Lee, M.A.: *Astrophys. J.* **646**(2), 1319 (2006)
- Tylka, A.J., et al.: CP528: Acceleration and transport of energetic particles observed in the heliosphere. In: Mewaldt, R.A., et al. (eds.) ACE 2000 Symposium, California, January 2000. AIP Conf. Proc., vol. 528, p. 147. AIP, New York (2000)
- Tylka, A.J., et al.: *Astrophys. J.* **625**, 474 (2005)
- Tylka, A.J., et al.: *Sol. Phys.* **285**, 251 (2013)
- Wibberenz, G., Cane, H.V.: *Astrophys. J.* **650**, 1199 (2006)
- Wiedenbeck, M.E., et al.: *Astrophys. J.* **762**, 54 (2013)
- Wild, J.P., et al.: *Annu. Rev. Astron. Astrophys.* **1**, 291 (1963)
- Wilson, J.W., et al. (ed.): Shielding strategies for human space exploration, NASA Conference Publication, 3360 (1997)
- Xapsos, M.A., et al.: *IEEE Trans. Nucl. Sci.* **59**(4), 1054 (2012)
- Zank, G.P., et al.: *Astrophys. J.* **797**, 28 (2014)

Zank, G.P., et al.: *Astrophys. J.* **814**, 137 (2015a)

Zank, G.P., et al.: AIAC '14: linear and nonlinear particle energization throughout the heliosphere and beyond. In: Zank, G.P. (ed.) 14th Annual International Astrophysics Conference, Florida, April 2015. *J. Phys.: Conc. Ser.*, vol. 642, p. 012031. IOP Publishing, USA (2015b)

Zeitlin, C., et al.: *Science*. **340**(6136), 1080 (2013)

Open Access This chapter is licensed under the terms of the Creative Commons Attribution 4.0 International License (<http://creativecommons.org/licenses/by/4.0/>), which permits use, sharing, adaptation, distribution and reproduction in any medium or format, as long as you give appropriate credit to the original author(s) and the source, provide a link to the Creative Commons license and indicate if changes were made.

The images or other third party material in this chapter are included in the chapter's Creative Commons license, unless indicated otherwise in a credit line to the material. If material is not included in the chapter's Creative Commons license and your intended use is not permitted by statutory regulation or exceeds the permitted use, you will need to obtain permission directly from the copyright holder.

